research papers

A cell for the *in situ* study of electrocrystallization

Andrew Parkin,* Stuart F. Johnstone, Andrew R. Mount, Simon Parsons,* Colin R. Pulham and David Sanders

School of Chemistry, University of Edinburgh, Kings Buildings, West Mains Road, Edinburgh EH9 3JJ, Scotland, UK. Correspondence e-mail: andrewp@chem.gla.ac.uk, s.parsons@ed.ac.uk

A new cell for studying electrocrystallization *in situ* on a diffractometer is reported. The construction of the cell is described in detail. The working electrode, fabricated from a propelling pencil lead encased in glass, was designed to sit in the path of the incident X-ray beam so that processes occurring at its tip could be studied using diffraction methods. Practical difficulties of both design and data collection are discussed, as well as advantages and limitations of the method. In a series of proof-of-concept experiments, the cell has been applied to the *in situ* study of silver, both by powder and single-crystal methods. A new silver oxide perchlorate phase, $Ag_7O_8ClO_4$, was also identified using the cell; use of the same growth conditions *ex situ* enabled a sample of this new phase to be isolated.

1. Introduction

X-ray diffraction techniques are most frequently applied to materials that have been prepared remotely from the diffractometer. The widespread use of area detectors now makes it possible to study processes as they occur, and such *in situ* methods have been applied to a variety of systems. Notable examples of this type of work are the time-resolved powder diffraction studies of intercalation reactions (*e.g.* Fogg & O'Hare, 1999) and the study of metastable excited states (Coppens, 2003). *In situ* methods have also been applied by several groups to crystal growth of compounds which are liquids at room temperature and pressure (Bond, 2003; Bond & Parsons, 2002; Pardoe *et al.*, 2003; Boese *et al.*, 1999; Boese, Downs *et al.*, 2003; Boese, Kirchner *et al.*, 2003), with the laser-assisted crystal growth methods developed by Boese & Nussbaumer (1994) being particularly successful. Methods for crystal growth from liquids by application of high pressure have also been developed (Allan *et al.*, 1999, 2002).

Electrocrystallization enables the controlled synthesis of crystalline conducting materials when a redox-active species is soluble in one form and insoluble in another. Electrochemical conversion from the soluble to the insoluble form allows precise control of the nucleation and crystal growth rates. Although this method has been extensively applied, a more fundamental understanding of the crystal growth process is desirable; a review on nucleation and growth phenomena in the electrocrystallization of metals was published in 2000 (Budevski *et al.*, 2000).

In this paper we describe a new electrochemical cell designed to be accommodated on the goniometer head of a standard laboratory diffractometer, thereby allowing *in situ* experiments which can combine electrochemical techniques with X-ray diffraction studies. Previous papers describing *in situ* X-ray diffraction experiments have focused on the structural changes observed on the electrode surface by using X-

ray surface techniques, such as SEXAFS and XANES (Fleischmann *et al.*, 1986), or on grain-growth kinetics (Natter *et al.*, 2000). Very recently an *in situ* cell for long-term diffraction experiments involving small-angle scattering, powder diffraction and absorption spectroscopy has been described (Braun *et al.*, 2003). Recent advances in single-crystal diffraction instrumentation and in techniques for dealing with data from twinned crystals mean that studying electrochemical crystal growth *in situ* using X-ray diffraction techniques has now become a subject area that is ripe for development and exploitation.

2. Experimental

Several criteria needed to be met in designing an electrochemical cell suitable for *in situ* X-ray diffraction studies. The cell was required to be sufficiently small and light so as to be mountable on an ordinary laboratory diffractometer (in this case a Bruker Smart Apex system). It had to be large enough to contain a sufficient volume of electrolyte and the working, counter and reference electrodes. The tip of the working electrode was to be centred in the X-ray path. The cell was constructed of amorphous materials, scattering from which would contribute only to the background of the diffraction pattern. Electrical connections between the cell and the power source needed to be flexible enough to allow rotation of the cell about the φ and ω axes of the diffractometer.

2.1. Construction of the cell

The base of the cell was formed from a standard B7 Quickfit extended cone with a taper drawn out to house a pencil lead which formed the working electrode (Fig. 1i). The electrode was cleaned by brief treatment with a flame, inserted into the taper, and glass was melted onto it to form a reasonably tight (though in practice not watertight) fit between the rod and the

glass. A 1 cm length of 3 mm (outer diameter, o.d.) glass rod was attached to the bottom of the cone as a mount. A hole was blown in the side of the cone between the mount and the ground-glass joint. The electrical connection between the working electrode and the power source was established by inserting a wire (insulated with heat-shrink plastic) into molten gallium contained in the hollow centre of the cell base. The sizes of all the components of the base were important as the tip of the working electrode was to be centred in the X-ray beam; typical dimensions used in this study are given in Figs. 1(i) and 1(ii). The top part of the cell, designed to contain the electrolyte and the counter and reference electrodes, was formed from two standard Quickfit sockets (one B7 and one B10) joined by approximately 1 cm length of 5 mm (o.d.) NMR tube (Fig. 1iii).

The cell was glued into a light magnetic Z platform (as supplied by Hampton Research, part number HR4-653) with the magnet drilled out and mounted on a short XYZ goniometer head (height 27.5 mm), also supplied by Hampton
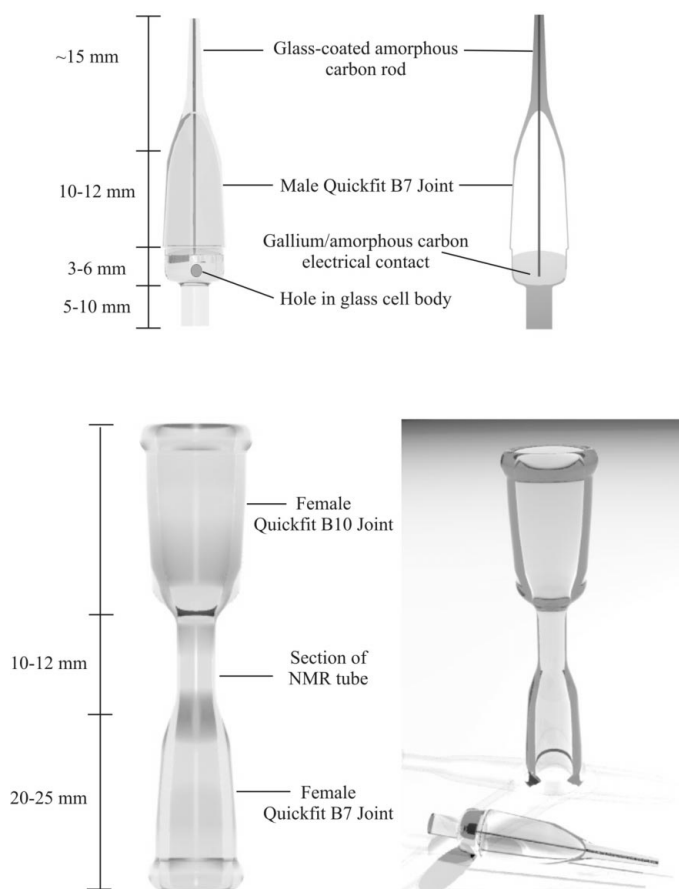
Figure 1
The design dimensions of the electrocrystallization cell. Top left: the base and working electrode assembly. The electrode is constructed from amorphous carbon rod coated in glass leaving the extreme tip exposed. Top right: a cross section of the base showing the electrical contact between the gallium and the working electrode. Bottom left: the upper part of the cell, which contains the electrolyte and the reference and counter electrodes. Bottom right: upper and lower components of the cell showing relative dimensions.

Research. Illustrations of both these components are available on the Hampton Research Website (www.hamptonresearch.com). This specific assembly provides excellent height flexibility and ensures that the tip of the electrode can be positioned in the incident beam path. A view of the cell mounted on the diffractometer is shown in Fig. 2.

A three-electrode configuration was used throughout with silver counter and reference electrodes. All experiments were performed potentiostatically using an Oxford Electrodes modular potentiostat, with current and voltage data collected on a PC. The charge passed was determined by integration of the current-*versus*-time profile.

2.2. General experimental details

All chemicals were obtained from Sigma-Aldrich and used as received.

Diffraction data were collected at room temperature on a Bruker Smart Apex diffractometer equipped with a sealed-tube Mo $K\alpha$ X-ray source and a locally constructed short collimator of length 12.3 cm. The sample to detector distance was 8 cm to prevent collisions with the top of the cell as it was rotated around ω. The size of the cell would necessitate the use of a modified beam stop, but we found it more convenient simply to remove the beam stop, and position the 2θ arm so that the direct beam did not hit the detector. Note that it is essential to scan around the diffractometer cabinet with a radiation monitor to ensure that no X-radiation has leaked into the laboratory. The crystal to detector distance was calibrated with a sample of polycrystalline silicon. Data were collected using the program *SMART* and processed using *GADDS* (for powder data) or *SAINT* (for single-crystal data) (all programs supplied by Bruker, 2000–2003). Absorption
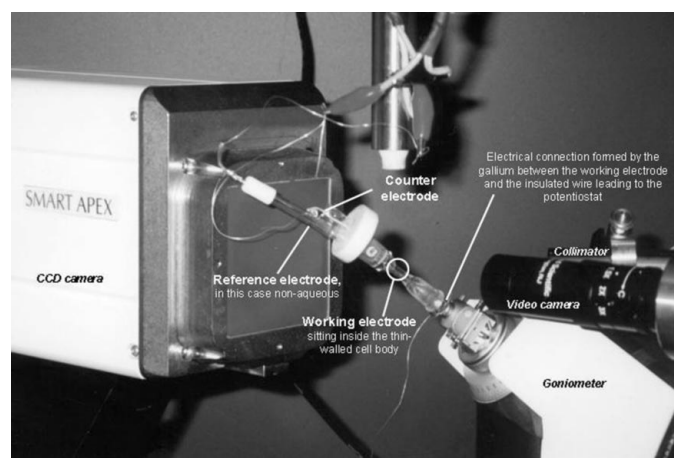
Figure 2
Photograph of the *in situ* cell mounted on the Bruker SMART APEX CCD diffractometer. The cell is supported by a short XYZ goniometer head to position the exposed-tip working electrode in the X-ray beam. It is pictured with a long non-aqueous reference electrode and a silver counter electrode. All wires leading from the three electrodes are insulated by heat-shrink tubing to prevent the circuit being shorted. The low-temperature device nozzle seen in the photograph provides a convenient mount for electric leads.

Table 1
Single-crystal refinement data for Ag and $Ag_7O_8ClO_4$.

	Silver	*In situ* $Ag_7O_8ClO_4$	*Ex situ* $Ag_7O_8ClO_4$
Formula	Ag	$Ag_7O_{12}Cl$	$Ag_7O_{12}Cl$
Molecular weight	107.87	982.54	982.54
Space group	$Fm\bar{3}m$	$Fm\bar{3}m$	$Fm\bar{3}m$
a (Å)	4.18 (2)	9.93 (2)	9.955 (6)
V (Å)	73.2 (4)	979 (2)	986.5 (6)
No. reflections for cell	24 ($8.4 < \theta < 26.3°$)	40 ($8.2 < \theta < 28.0°$)	928 ($8.2 < \theta < 29.7°$)
$2\theta_{max}$ (°)	52.38	55.82	61.04
Z	4	4	4
D_c (Mg m^{-3})	9.786	6.668	6.615
μ (mm^{-1})	26.004	14.053	13.943
Reflections collected	25	159	1447
No. of unique data (R_{int})	10; 8 used in refinement (0.31)	75 (0.0303)	99 (0.0209)
Data with $I > 2\sigma(I)$	10	54	98
T_{min}, T_{max}	0.172, 1.000	0.334, 1.000	0.577, 1.000
Parameters/restraints	1/0	9/0	9/0
R_1 [$F > 4\sigma(F)$]	0.066	0.0767	0.0214
R_1 (all data)	0.066	0.0982	0.0216
wR_2 (F^2, all data)	0.165	0.1920	0.0625
S	1.670	1.173	1.181
Extinction coefficient	0	0.0063 (14)	0.00119 (14)
$(\Delta/\sigma)_{max}$	0.000	0.000	0.000
$\Delta\rho_{max}, \Delta\rho_{min}$ (e Å^{-3})	1.33, −2.17	2.995, −3.234	1.527, −0.864
Data completeness (θ_{full})	1.000 (26.19)	0.852 (27.91)	0.917 (30.57)
Data:parameter ratio	8:1	6:1	9.8:1

corrections were applied to single-crystal data sets with the multiscan procedure *SADABS* (Sheldrick, 2002).

2.3. Identification of an electrochemically produced powder

The cell was filled with a 0.2 *M* aqueous solution of $AgClO_4$ [prepared using silver perchlorate hydrate (0.46 g) in distilled water (10 cm^3)]. The carbon working electrode, silver counter electrode and silver pseudo-reference electrode were attached to the potentiostat, and a reductive potential of −1.5 V was applied to the working electrode for 120 min, and then at −2.0 V for 30 min. Rotation images were taken initially and then after 15, 45 and 150 min deposition time (Figs. 3i–3iv, respectively), corresponding to total charge passed of −6.5, −20 and −105 mC, respectively. A 60 s rotation photo after 15 min (Fig. 3ii) showed the peaks attributable to diffraction from the {111} and {200} planes of the silver (*Fm$\bar{3}$m*, a = 4.0862 Å; Swanson & Tatge, 1953), observed at $2\theta = 17.6$ and 20.6°, with one higher angle peak being faintly visible at $2\theta = 33.9°$ due to the 311 reflection. After 45 min (Fig. 3iii) a peak at $2\theta = 28.5°$, the 220 reflection, could be discerned, but the line at 33.9° was still only faintly visible. After 150 min, a 300 s exposure gave the first eight peaks at $2\theta = 17.6$, 20.6, 28.5, 33.9, 35.5, 41.0, 44.8 and 46.2° (literature values: 17.3, 20.0, 28.5,

33.5, 35.1, 40.8, 44.5, 45.7°; Fig. 3v). No refinement was performed against the integrated patterns.

2.4. Growth and identification of a single-crystal

The cell was filled with a 0.2 *M* electrolytic solution of $AgClO_4$ (prepared as described above). The carbon working electrode, silver counter electrode and silver reference electrode were attached to a potentiostat, and a reductive potential of −0.1 V was maintained over the system for 60 min, passing a total charge of −2.4 mC. It was clear from the diffraction pattern that only a few small single crystallites were present, and a data set was collected, rotating 180° through φ in 0.36° steps. One orientation matrix was determined using *GEMINI* (Sparks, 2000), and a further 12 using *CELL_NOW* (Sheldrick, 2002). The data set was integrated using one of these matrices, and an absorption correction applied using *SADABS* (Sheldrick, 2002). The scale factor was
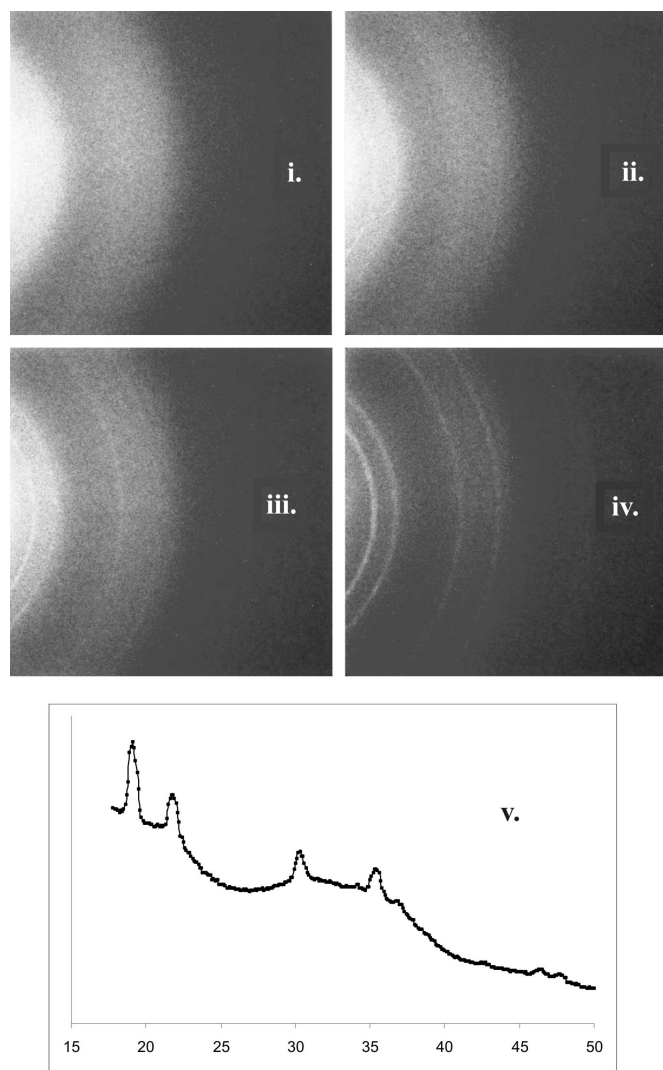
Figure 3
Powder patterns of silver deposited electrochemically on the surface of the graphite working electrode; 60 s rotation frames after 0 (i), 15 (ii), 45 (iii) and 150 (iv) min. (v) The integrated powder pattern of a 300 s rotation frame taken after 150 min of silver deposition.

refined against $|F|^2$ (*CRYSTALS*; Watkin *et al.*, 2003) with the isotropic displacement parameter of Ag fixed at 0.025 (Simerskà, 1961). The 002 and 111 reflections were omitted from the refinement as they appeared to suffer from extinction. The final conventional R factor (based on $|F|$) was 0.066; other data collection and refinement statistics are listed in Table 1.

2.5. Comparison of data collection strategies based on φ and ω scans

The aim of this experiment was to compare the effect of collecting diffraction data in ω or φ mode on single-crystal diffraction data quality. Data were collected at room temperature with a crystal of silicon ($1.0 \times 0.3 \times 0.2$ mm) mounted in the electrochemical cell, which was filled with water to simulate more closely likely experimental conditions. Two data sets were collected by scanning through 180° in 500 0.36° steps in ω and φ. The data were integrated to $2\theta_{max} = 50°$. 81 reflections were measured in the ω-scan data collection, and these merged to yield 12 independent data with a very high $R_{int} = 0.687$. In the φ-scan experiment, 45 reflections were measured, again yielding 12 unique data, but this time with $R_{int} = 0.091$. Multiscan absorption correction was carried out using *SADABS*; the maximum orders of the odd and even spherical harmonics were limited to one and two, respectively, because of the small number of data available. The ratios of $T_{min}:T_{max}$ were 0.35 and 0.80 for the ω and φ data sets, respectively; the values R_{int} after correction were 0.071 (ω) and 0.002 (φ). The structure of Si was refined against these two data sets (*CRYSTALS*; Watkin *et al.*, 2003). The isotropic displacement parameter of the silicon was fixed at 0.004 (calculated from the Debye temperature; Als-Neilsen & McMorrow, 2001), and the extinction parameter (Larson, 1970) was restrained to be 300 (50); the scale factor was refined freely; refinements were carried out *versus* $|F|^2$ with statistical weights. Reflections 222, 244 and 226 were omitted as these cannot be modelled with spherical atom scattering factors. For the refinement against the ω-scan data set, three further outlying reflections were also omitted. For the ω-scan data set, $R(F) = 0.044$, $wR(F^2) = 0.110$, $S = 1.30$ for nine data and two parameters; corresponding data for the φ set were 0.031, 0.082 and 1.04 for 12 data and two parameters.

2.6. Growth and identification of $Ag_7O_8ClO_4$

The cell was filled with an electrolytic solution of 0.1 M of $AgClO_4$ and 2 M of $NaClO_4$ [prepared from $AgClO_4$ hydrate (0.47 g) and $NaClO_4$ (2.23 g) in distilled water (10 cm^3)]. An oxidative potential of 0.5 V was applied, leading to the formation of a black solid. The diffraction pattern of the solid could be indexed after only 20 min, though growth was allowed to proceed for a total of 150 min. A data set was collected by rotation through 180° in φ, and an absorption correction applied using *SADABS*. The structure was solved by direct methods using in space group $Fm\bar{3}m$, and refined using full-matrix least squares on $|F|^2$ using *SHELXTL* (Sheldrick, 2001). The perchlorate anion, which is disordered

about an $m\bar{3}m$ site, was modelled as a rigid group. U_{iso} for the chlorine atom was fixed at 0.05 Å^2 and for the oxygen atoms at 0.06 Å^2. The final conventional R factor was 7.67%. A second crystal was grown under the same conditions over a period of 150 min *ex situ*, and a single crystal was cut from the deposit produced. A data set was collected using conventional procedures at room temperature. The structural model described above, when refined against this data set, yielded an R factor of 2.14%. Crystal data are given in Table 1; atomic coordinates derived from the *ex situ* study are available in the supplementary material.[1]

3. Discussion

3.1. Electrode design

Electrochemical cells used for electroanalysis, electrocrystallization and a variety of other applications typically contain three electrodes. The electrochemical reaction of interest occurs at the working electrode. In a potentiostatic experiment electric current passes between the working and counter electrodes, and constant potential is maintained relative to the reference electrode. All three electrodes must lie in the electrolyte. In this paper we describe the construction of a glass cell which can be mounted on a diffractometer, and is suitable for *in situ* monitoring of an electrochemical process occurring at the working electrode (Fig. 1).

Although the counter and reference electrodes may lie anywhere in the cell, and can be made of any material, the working electrode encountered the incident X-ray beam, and so it contributed to the measured diffraction pattern. The most commonly used material for working electrodes is platinum, but this tends to be highly crystalline, and would likely produce a high background in the form of powder rings, as well as strongly absorbing the incident radiation. A more suitable material is an amorphous form of graphitic carbon. A convenient and inexpensive electrode can be constructed using a 'lead' refill for a propelling pencil. Pencil leads contain polymer added to control the hardness of the lead, and this removes virtually all of the crystallinity of the graphite, and scattering of the incident X-ray beam only contributes to the overall background of the diffraction pattern (Fig. 3i). Although addition of the polymer means that the electrode has significant resistance (compared with pure graphite), this was found not to impede the electrocrystallization experiments performed in this study.

Coating the lead in glass strengthens the electrode and limits the site of electrochemical processes to the tip of the electrode, where it can be sampled by the X-ray beam. Prior to coating with glass it is necessary to flame-clean the electrode; pencil leads supplied by Staedtler were found to explode during this operation, but those supplied by Linex were suitable. The electrode material does not 'take' the glass coating perfectly, and some leakage of the electrolyte occurs

---

[1] Supplementary data are available from the IUCr electronic archives (Reference: HE5276). Services for accessing these data are described at the back of the journal.

between the glass coating and the electrode. Inevitably, therefore, some electrochemical processes occur in this region, though this did not prove to be especially problematical. An advantage of the strengthening given by the glass covering was that the surface of the electrode could be cleaned and freshened after use by rubbing with sandpaper. The tip of the electrode should have a small surface area to limit the possible nucleation sites for crystal growth. An electrode diameter of 0.1 mm or less is ideal, with only the flat top surface of the electrode being exposed. The narrowest commercial leads are 0.3 mm o.d., but the tip can be tapered to a narrow point using sandpaper.

Electrical connections are usually formed by wires attached to the base of a working electrode. In this application it was difficult to attach a wire directly to the graphite rod, which was quite fragile. The base of the electrode therefore consisted of a chamber containing gallium into which both the electrode and the insulated connecting wire leading to the potentiostat were inserted. The gallium in the cell could be melted to maintain the electrical contact between the wire and the fragile working electrode. Gallium has a tendency to cling to dirty surfaces; to avoid this the cell was freshly glass-blown and the working electrode flame-cleaned immediately prior to inserting the gallium in the cell body. To provide sufficient orientational flexibility during diffraction data collection, fine wire sealed with heat-shrink tubing was used for electrical connections to all three electrodes. These wires intertwine without shorting the circuit and the cell could rotate about ω and φ.

The electrolyte was contained in a reservoir formed by two female ground glass joints connected by a short length of NMR tubing. One joint fitted over the top of the assembly containing of the working electrode and its associated electrical connections, the other joint accepted the counter and reference electrodes. The short length of NMR tube was positioned to surround the tip of the working electrode, minimizing the path length of the incident and diffracted X-ray beams through the glass of the cell wall and the electrolyte. Standard 5 mm NMR tubing was robust enough to support the weight of the cell, and was broad enough to prevent the electrochemical reaction being limited by diffusion control.
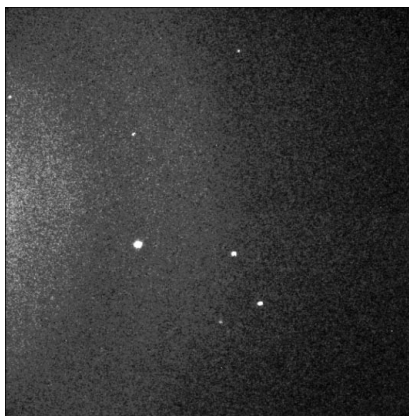
Figure 4
Single-crystal diffraction pattern obtained during data collection of crystalline $Ag_7O_8ClO_4$ grown using the *in situ* electrocrystallization cell.

Thin-walled NMR tubes would contribute less to background scattering, but were found to be too fragile and difficult to manipulate during glass-blowing. The cell can be readily disassembled to permit cleaning of the working electrode and other components.

The Bruker SMART diffractometer has a fixed χ circle at 54.79°, and the cell was therefore positioned at an angle (Fig. 2). If the volume of the upper reservoir was too large then the cell became overly top-heavy, and became miscentred over the course of an experiment. This may be less of an issue on other diffractometers where χ can be fixed at zero. The overall volume of the cell was around 1 cm^3, and in some experiments this could limit the supply of the electroactive species under investigation in solution.

3.2. Growth and characterization of polycrystalline samples

Although they are usually primarily designed for single-crystal diffraction studies, CCD instruments can be used to investigate polycrystalline samples to yield data suitable for phase identification, and even Rietveld refinement. Until precise crystal growth conditions have been optimized, electrochemical experiments produce powders instead of single crystals, and it would be an advantage if the cell could be used to identify simple polycrystalline samples. In order to prove that this is feasible we have identified a sample of silver grown in the *in situ* electrochemical cell described in the previous section. Silver is certainly a very favourable system for such a preliminary study: it has a simple crystal structure (cubic, $Fm\bar{3}m$) and scatters X-rays powerfully.

A sample of silver was deposited on the working electrode by electrochemical reduction of an aqueous solution of silver perchlorate. Rotation photographs were acquired before deposition and then after 15, 45 and 150 min. Despite the high amorphous background scattering contributed by the cell (Fig. 3i), even a small amount of electrodeposited silver yielded an observable pattern. Figs. 3(ii)–3(iv) show the development of the powder pattern as a function of deposition time. Even after only 15 min of electrodeposition, which can be calculated to result in a deposit of 7.5 µg of Ag, the first two lines of the silver diffraction pattern were visible (Fig. 3ii); after 150 min the first eight lines of the pattern could be discerned (Figs. 3iv and 3v). Changing the contrast of the images assisted in locating weak diffraction peaks.

The use of a lower potential (and hence current density) resulted in slow deposition of silver, forming dendrimers because it is thermodynamically more favourable for the silver to form on a silver surface than on carbon. At higher potentials and currents, however, the process becomes kinetically controlled, giving more uniform surface coverage. It proved possible to control the growth to such an extent that only a few relatively large crystallites were formed (this can be rapidly assessed using static or 'still' exposure). The diffraction pattern of this sample was measured using single-crystal data collection procedures. It proved possible to index the strongest peaks in the pattern on the basis of 13 different orientation matrices using the programs *GEMINI* and
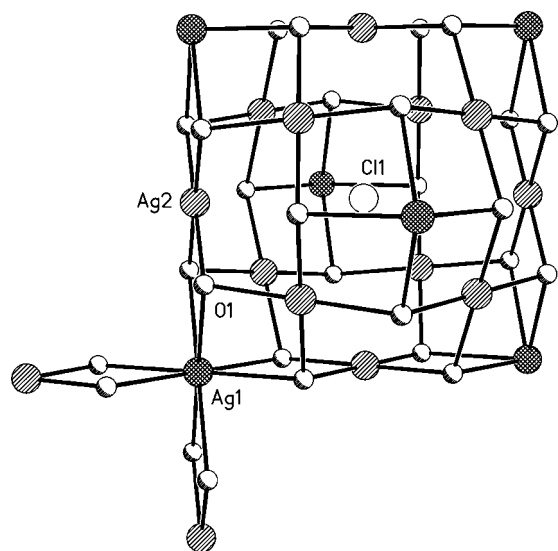
Figure 5
$Ag_7O_8ClO_4$. Ag1 and Ag2 are eight- and four-coordinate, respectively. The perchlorate anion is disordered; only the Cl position is shown.

CELL_NOW. Refinement of the crystal structure of silver against single-crystal diffraction intensities extracted on the basis of one of these matrices yielded an R factor of 8.63%.

It is clear that the powder data measured in this study are by no means of high enough quality to index, solve and refine an unknown structure. Complex powder patterns would be difficult to identify, especially if the diffraction profiles were broad. This procedure is most suitable as a phase identification tool for materials formed under varying electrochemical conditions (*e.g.* distinguishing between a number of phases of a material by the presence or absence of certain unique peaks). Careful deposition can yield samples which can be treated using single-crystal methods, and under these circumstances the cell has much greater potential for the full structural characterization of new phases.

3.3. Single-crystal data collection: comparison of ω- and φ-scan strategies

On a fixed-χ instrument such as the Bruker Smart single-crystal diffractometer, data may be collected using either ω or φ scans. During ω scans with χ fixed at 54.79°, the path length of the X-rays through the cell can vary substantially, and this introduces a significant systematic error into the data set. The cell was constructed using a 5 mm NMR tube; these are of uniform thickness to ensure field isotropy and to enable spinning during NMR experiments. Absorption anisotropy from the cell is thus minimized if the data collection is carried out using a φ rotation with the axis of the cell perpendicular to the X-ray beam.

In order to assess the magnitude of this effect, a single crystal of silicon was mounted in the cell and two data sets were collected, one using ω scans, the other using φ scans. The values of R_{int} (prior to any absorption correction) were 0.69 and 0.09 for the data sets collected using ω and φ scans, respectively, though these were reduced to 0.07 and 0.00 after

application of a multiscan absorption correction (*SADABS*). This procedure corrected not only for absorption anisotropy arising from the cell, but also for that arising from the silicon sample. Refinement of the silicon structure (Batchelder & Simmons, 1964) against these data sets converged to conventional R factors of 0.044 and 0.031 for the ω and φ data sets, respectively.

In the case of the small data sets obtained here, only limited expansions of spherical harmonics were used in the multiscan absorption correction, and even here it is likely that the φ-scan data set has been over-corrected. In data sets with larger numbers of reflections (such as that obtained for $Ag_7O_8ClO_4$; see below) an absorption correction using this procedure would be more routinely applicable. The values of R_{int} prior to correction for absorption indicate that the much smaller systematic errors incurred by collecting data in φ mode makes this the preferred choice for single-crystal data collection using the cell described here.

3.4. Growth and identification of $Ag_7O_8ClO_4$

The identification of the product of an electrocrystallization experiment is usually made after recovery of a crystal from the electrochemical cell after crystal growth. The *in situ* electrochemical cell described in this paper is designed to permit characterization of the product of an experiment while it is taking place.

When using the *in situ* electrocrystallization cell, diffraction spots may be observed after only a few minutes. Standke & Jansen (1985, 1986) have described the formation of Ag_2O_3 and Ag_3O_4 by slow oxidative electrocrystallization from aqueous silver perchlorate. During an investigation into this process it was possible to index a diffraction pattern after only 20 min of crystal growth, and it was immediately clear that a new phase had been formed. After 150 min of crystal growth it was possible to collect a data set (using φ scans as described above); a view of one frame taken during the data collection is shown in Fig. 4.

Structure solution by direct methods identified the new phase as $Ag_7O_8ClO_4$, and refinement converged to 7.67%. When the same conditions which generated this new phase were applied to an *ex situ* growth experiment, and a crystal recovered and data collected according to more conventional procedures, it was possible to refine the structure to an R factor of 2.14%.

The crystal structure of $Ag_7O_8ClO_4$ consists of a three-dimensional $Ag_7O_8^+$ network with holes in the lattice occupied by the perchlorate anions (Fig. 5). This arrangement has been observed previously with nitrate, fluoride or fluoroborate (Robin *et al.*, 1966) anions sitting in the holes, although some doubt has been expressed that larger anions could be so accommodated. These salts have been shown to be superconducting at low temperature. One of the seven silver atoms in the formula unit is eight-coordinate (Ag1) and the remainder are four-coordinate (Ag2). The Ag1—O1 and Ag2—O1 bond lengths are 2.424 (5) and 2.0812 (17) Å, respectively, in agreement with results obtained for the other

salts. The perchlorate is disordered about an $m\bar{3}m$ special position.

Crystal growth of $Ag_7O_8ClO_4$ was accompanied by parallel evolution of hydrogen at the counter electrode and oxygen at the working electrode by electrolysis of the water. With the cell mounted at $\chi = 54.74°$, some crystallites were dislodged by gas evolution. In the *ex situ* experiment in which the cell was held vertically, this did not occur, and it may be that $\chi = 0$ geometry is preferable for this kind of experiment. Minimizing the surface area of the working electrode can also promote single-crystal growth, as opposed to powder growth, by reducing the number of nucleation sites. This cell used throughout this study had an electrode diameter of 0.3 mm, but in more recent work we have used an electrode of diameter 0.07 mm.

4. Conclusions

We have described in this paper a new cell which is suitable for the study of electrochemical processes by *in situ* X-ray diffraction. The cell has been successfully applied to two single-crystal investigations: one proof-of-concept experiment on silver, the other leading to the identification of a new silver oxide perchlorate phase. Although deposits rarely contain only one crystal, modern software is able to index the complex diffraction patterns obtained. Powder diffraction experiments have been shown to be useful for phase identification, although only a rather simple example has thus far been investigated. We anticipate that this cell will be especially useful for the optimization of electrochemical crystal growth conditions, for the study of unstable or air-sensitive systems, and the investigation of single-crystal to single-crystal junctions.

References

Allan, D. R., Clark, S. J., Dawson, A., McGregor, P. A. & Parsons, S. (2002). *J. Chem. Soc. Dalton Trans.* pp. 1867–1871.

Allan, D. R., Clark, S. J., Ibberson, R. M., Parsons, S., Pulham, C. R. & Sawyer, L. (1999). *Chem. Commun.* pp. 751–752.

Als-Neilsen, J. & McMorrow, D. (2001). *Elements of Modern X-ray Physics*. New York: Wiley.

Batchelder, D. N. & Simmons, R. O. (1964). *J. Chem. Phys.* **41**, 2324–2329.

Boese, R., Downs, A. J., Greene, T. M., Hall, A. W., Morrison, C. A. & Parsons, S. (2003). *Organometallics*, **22**, 2450–2457.

Boese, R., Kirchner, M. T., Billups, W. E. & Norman, L. R. (2003). *Angew. Chem. Int. Ed. Engl.* **42**, 1961–1963.

Boese, R. & Nussbaumer, M. (1994). *Correlations, Transformations, and Interactions in Organic Crystal Chemistry*, edited by D. W. Jones & A. Katrusiak, *IUCr Crystallographic Symposia*, Vol. 7, pp. 20–37. Oxford University Press.

Boese, R., Weiss, H.-C. & Blaser, D. (1999). *Angew. Chem. Int. Ed. Engl.* **38**, 988–992.

Bond, A. D. (2003). *Chem. Commun.* pp. 250–251.

Bond, A. D. & Parsons, S. (2002). *Acta Cryst.* E**58**, o550–o552.

Braun, A., Shrout, S., Fowlks, A. C., Osaisai, B. A., Seifert, S., Granlund, E. & Cairns, E. J. (2003). *J. Synchrotron Rad.* **10**, 320–325.

Bruker (2000–2003). *SMART, SAINT, GADDS*. Programs for diffractometer control and data processing. Bruker AXS, Madison, Wisconsin, USA.

Budevski, E., Staikov, G. & Lorenz, W. J. (2000). *Electrochim. Acta*, **45**, 2559–2574.

Coppens, P. (2003). *Chem. Commun.* pp. 1317–1320.

Fogg, A. M. & O'Hare, D. (1999). *Chem. Mater.* **11**, 1771–1775.

Fleischmann, M., Oliver, A. & Robinson, J. (1986). *Electrochim. Acta*, **31**, 899–906.

Larson, A. C. (1970). *Crystallographic Computing*, edited by F. R. Ahmed, S. R. Hall & C. P. Huber, pp. 291–294. Copenhagen: Munksgaard.

Natter, H., Schmelzer, M., Löffler, M.-S., Krill, C. E., Fitch, A. & Hempelmann, R. (2000). *J. Phys. Chem. B*, **104**, 2467–2476.

Pardoe, J. A. J., Norman, N. C., Timms, P. L., Parsons, S., Mackie, I., Pulham, C. R. & Rankin, D. W. H. (2003). *Angew. Chem. Int. Ed. Engl.* **42**, 571–573.

Robin, M. B., Andres, K., Geballe, T. H., Kuebler, N. A. & McWhan, D. B. (1966). *Phys. Rev. Lett.* **17**, 917–919.

Sheldrick, G. M. (2001). *SHELXTL*. Version 6.12. University of Göttingen, Germany.

Sheldrick, G. M. (2002). *CELL_NOW* and *SADABS* (Version 2.04). University of Göttingen, Germany.

Simerská, M. (1961). *Acta Cryst.* **14**, 1259–1262.

Sparks, R. A. (2000). *GEMINI*. Version 1.05. Program for indexing diffraction patterns from twinned crystals. Bruker AXS, Madison, Wisconsin. USA.

Standke, B. & Jansen, M. (1985). *Angew Chem. Int. Ed. Engl.* **24**, 118–119.

Standke, B. & Jansen, M. (1986). *Angew Chem. Int. Ed. Engl.* **25**, 77–78.

Swanson, H. E. & Tatge, E. (1953). *National Bureau of Standards Report*, 539, 1-1, ICSD collection code 64706.

Watkin, D. J., Prout, C. K., Carruthers, J. R., Betteridge, P. W. & Cooper, R. I. (2003). *CRYSTALS*. Issue 12. Chemical Crystallography Laboratory, University of Oxford.